

Updated analysis of πN elastic scattering data to 2.1 GeV: The baryon spectrum

Richard A. Arndt, Igor I. Strakovsky,* and Ron L. Workman

Department of Physics, Virginia Polytechnic Institute and State University, Blacksburg, Virginia 24061

Marcello M. Pavan

University of British Columbia, Vancouver, British Columbia, Canada V6T 2A3

(Received 26 May 1995)

We present the results of energy-dependent and single-energy partial-wave analyses of πN elastic scattering data with laboratory kinetic energies below 2.1 GeV. Resonance structures have been extracted using Breit-Wigner fits, speed plots, and a complex plane mapping of the associated poles and zeros. This is the first set of resonance parameters from a VPI analysis constrained by fixed- t dispersion relations. We have searched our solutions for structures which may have been missed in our previous analyses, finding candidates in the S_{11} and F_{15} partial-wave amplitudes. Our results are compared with those found by the Karlsruhe, Carnegie-Mellon-Berkeley, and Kent State groups.

PACS number(s): 14.20.Gk, 13.30.Eg, 13.75.Gx, 11.80.Et

I. INTRODUCTION

We have performed a partial-wave analysis of pion-nucleon elastic scattering data up to a laboratory pion kinetic energy of 2.1 GeV. This work supersedes our last published analysis [1] (named SM90). The present analysis (called SM95) was performed on a larger data base, and was constrained by fixed- t dispersion relations (FTDR). In a previous study [2] (solution FA93) employing FTDR, we focused on a determination of the pion-nucleon coupling constant ($g^2/4\pi$), finding the value $g^2/4\pi = 13.75 \pm 0.15$. In the present study we concentrate on the baryon spectrum as determined by Breit-Wigner fits, speed plots, and complex plane mappings. As our algorithm for implementing FTDR constraints has been described in Ref. [2], we will only outline the method in this paper. One further change in our method of analysis was made in response to a suggestion made by Höhler [3]. We have scanned our energy-dependent solution for "missing" structures by sweeping an adjustable Breit-Wigner resonance contribution through each partial wave. As a result, we have found some evidence for a small number of additional structures.

In Sec. II, we will briefly describe the additions made to our database since the publication of Ref. [1]. In Sec. III, we will review the basic formalism [1,2,4] used in our analyses. Results for the baryon spectrum and associated couplings will be given in Sec. IV. Here we will also compare the present solution with the older solution SM90. Finally, in Sec. V, we will compare our resonance spectrum with the results of the Karlsruhe [5–7], Carnegie-Mellon-Berkeley (CMB) [8], and Kent State [9] groups. In particular, we will comment on discrepancies in the observed resonance states.

II. THE DATABASE

Our previous published πN scattering analysis [1] (SM90) was based on 10031 $\pi^+ p$, 9344 $\pi^- p$, and 2132

charge-exchange data. Since then we have added 259 $\pi^+ p$, 691 $\pi^- p$, and 54 charge-exchange data. Some other measurements were removed [10] from the analyses in order to resolve database conflicts. The new low-energy πN data were produced mainly at the TRIUMF, LAMPF, and PSI meson facilities, and at the SPNPI and ITEP facilities in the 1 GeV region. The distribution of recent (post-1990) data is given schematically in Fig. 1.

Since most of the new data [11–25] are from high-intensity facilities, they generally have smaller statistical errors and thus have greater influence on the fits. A large fraction of the new $\pi^\pm p$ data were produced at energies spanning the Δ resonance. TRIUMF has produced differential cross sections with an accuracy of 1–2 % [14] and partial total cross sections [15,16]. LAMPF has produced a set of polarization parameters P , R , and A [23]. TRIUMF and LAMPF have produced total [16] and differential cross sections [17,21], and analyzing powers [22] for the charge exchange reaction. After a revised analysis and energy calibration, the Karlsruhe group, working at PSI, has provided a final set of both forward [20] and backward differential cross sections [18] and analyzing powers [25] at low energies.

Most of new $\pi^\pm p$ differential cross sections and analyzing powers above 780 MeV were measured at ITEP [11,12]. Some proton spin rotation parameters were measured below 600 MeV at SPNPI [19] and at 1300 MeV at ITEP [24].

Other experimental efforts will soon provide data in the low to intermediate energy region. A precise measurement of $\pi^\pm p$ elastic scattering cross sections was made in experiment (E645). This experiment covered the Δ isobar region and was completed at TRIUMF in the Summer of 1992 [26]. Partial total cross section measurements (E1190) for angles greater than 30° (lab) have been made at LAMPF in the Summers of 1991 and 1992 [27]. Data was taken between 40 and 500 MeV for $\pi^+ p$ and between 80 and 300 MeV for $\pi^- p$. In the spring of 1995 CHAOS, a new TRIUMF facility, began operating to measure polarization $\pi^\pm p$ data below 100 MeV (E560), and is expected to provide the first such measurements below 70 MeV [28]. A LAMPF experiment (E1178) will measure analyzing powers between 45 and 265

*On leave from St. Petersburg Nuclear Physics Institute, Gatchina, St. Petersburg, 188 350 Russia.

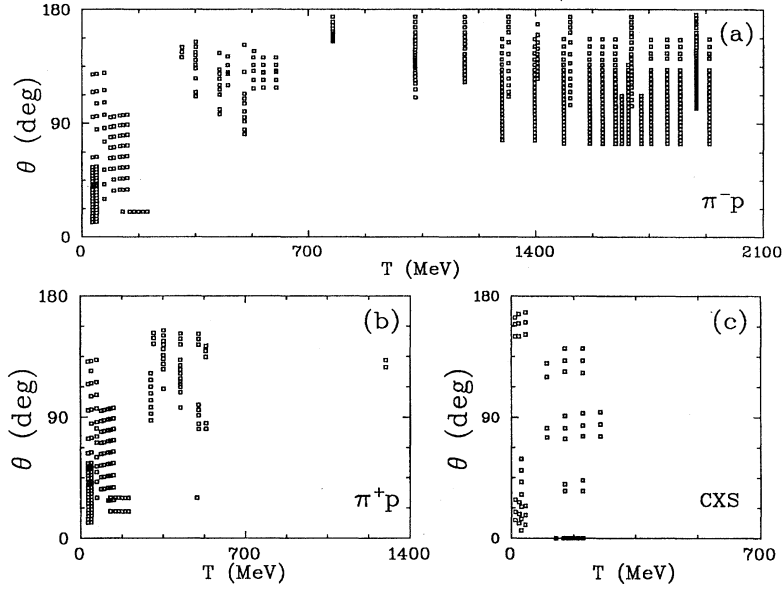


FIG. 1. Energy-angle distribution of recent (post-1990) (a) π^-p , (b) π^+p , and (c) charge exchange data. π^-p data are [observable (number of data)]: $d\sigma/d\Omega$ (249), P (326), partial total cross sections (6), R (55), and A (55). π^+p data are $d\sigma/d\Omega$ (109), partial total cross sections (12), P (56), R (41), and A (41). Charge exchange data are $d\sigma/d\Omega$ (24), total cross sections σ^{tot} (6), P (23). Total cross sections are plotted at zero degrees.

MeV for the charge exchange reaction in the Fall of 1995 [29].

The present solution (SM95) is compared with other recent VPI analyses in Table I. Here we display the quality of our fit to data in the different charge channels, as well as the number of searched parameters used in the fits.

III. FORMALISM

A. Chew-Mandelstam formalism

Our energy-dependent partial-wave fits are parametrized in terms of a coupled-channel Chew-Mandelstam K matrix, as described in Ref. [4]. The elastic scattering amplitude for each partial wave can be expressed in terms of a function \bar{K}

$$T_e = R_e \bar{K} / (1 - C_e \bar{K}) \quad (1)$$

with

$$\bar{K} = K_e + C_i K_0^2 / (1 - C_i K_i). \quad (2)$$

Here C_e and C_i are the Chew-Mandelstam elastic (πN) and inelastic ($\pi\Delta$) functions described in Ref. [4]; the elastic phase space factor, R_e , is the imaginary part of C_e . In order to control the behavior near the elastic threshold, the K -matrix elements (K_e , K_0 , and K_i) were expanded as polynomials in the energy variable $Z = (W_{\text{c.m.}} - W_{\text{th}})$, where

$W_{\text{c.m.}}$ and W_{th} are the center-of-mass and threshold energies, respectively, for elastic pion-nucleon scattering. Multiplying K_0 by an added factor of Z allowed the fixing of scattering lengths through the value of the leading term in K_e . It should be noted that the above $\pi\Delta$ channel is a “generic” inelastic channel. As in previous analyses, the S_{11} amplitude was given an additional ηN coupling. Charge splitting was accomplished through the multiplication of \bar{K} by an appropriate Coulomb barrier factor.

Single-energy analyses were parametrized as

$$S_e = (1 + 2iT_e) = \cos(\rho) e^{2i\delta}, \quad (3)$$

with the phase parameters δ and ρ expanded as linear functions around the analysis energy, and with a slope (energy derivative) fixed by the energy-dependent solution.

Details of the energy-dependent parametrization is as described in Ref. [4] with the following changes:

The subtraction point [4], W_Z , is now $M + \mu - 500$ MeV (M and μ being the nucleon and pion masses).

All K -matrix elements were expanded as energy polynomials except for an explicit K -matrix pole in the elastic component of the P_{33} partial wave.

The P_{33} was further modified for π^-p and charge exchange by scaling back the S -matrix modulus, η , to account for inverse pion-photoproduction around the resonance. This is similar to the method used by Tromborg *et al.* [30].

TABLE I. Comparison of present (SM95) and previous (FA93, SM90, and FA84) energy-dependent partial-wave analyses of elastic $\pi^\pm p$ scattering and charge-exchange (CX) data. N_{prm} is the number parameters ($l=1/2$ and $3/2$) varied in the fit.

Solution	Range (MeV)	χ^2/π^+p data	χ^2/π^-p data	χ^2/CX data	N_{prm}	Ref.
SM95	0–2100	22593/10197	18855/9421	4442/1625	94/80	Present
FA93	0–2100	23552/10106	20747/9304	4834/1668	83/77	[2]
SM90	0–2100	24897/10031	24293/9344	10814/2132	76/68	[1]
FA84	0–1100	7416/3771	10658/4942	2062/717	64/57	[4]

TABLE II. Table of χ^2 values for different minimal values of $g^2/4\pi$. The value of χ_{\min}^2 is given for different values of the GMO integral (J_{GMO}) and the a_{π^-p} scattering length.

$g^2/4\pi_{\min}$	$3a_{\pi^-p}$ (μ^{-1})	J_{GMO} (mb)	χ_{\min}^2
13.71	0.250	-1.00	46 381
13.75	0.250	-1.05	46 241
13.78	0.250	-1.10	46 370
13.72	0.255	-1.00	46 340
13.76	0.255	-1.05	46 236
13.81	0.255	-1.10	46 386
13.73	0.260	-1.00	46 287
13.77	0.260	-1.05	46 221
13.81	0.260	-1.10	46 422

Once an appropriate hadronic amplitude was determined, charge corrections were applied as described in Ref. [4].

Threshold behavior was determined in the following manner. The S -wave scattering lengths were linked to our dispersion relation constraints, as described below. The P -wave scattering volumes were searched without constraint. D waves were softly constrained to the Koch values [31], and the higher waves were fixed to Koch's results [31].

B. Dispersion relations constraints

Constraints on the partial-wave fits were generated from the forward C^\pm amplitudes and the invariant B amplitudes at fixed t in the range 0 to -0.3 (GeV/c)². (As mentioned in Ref. [2], the A^\pm dispersion relations, though not used as constraints, are quite well satisfied.) Reference [2] describes our method of applying forward and fixed- t dispersion relation constraints in order to generate solutions with fixed values of the pion-nucleon coupling constant, $g^2/4\pi$, and the isospin-even scattering length, $a^{(+)}$. In the present work we have generated a set of solutions in order to determine our sensitivity to choices of the π^-p scattering length and the pion-nucleon coupling constant. Table II displays the minimum value of χ^2 and $g^2/4\pi$ found in fits with different choices for the π^-p scattering length, a_{π^-p} , and the integral

$$J_{\text{GMO}} = \frac{1}{4\pi^2} \int \frac{\sigma_{\pi^-p} - \sigma_{\pi^+p}}{\omega} dk \quad (4)$$

which appears in the Goldberger-Miyazawa-Oehme (GMO) sum rule. Given a value for the integral, $a^{(-)}$ is directly related to the chosen value of $g^2/4\pi$.

Our final results were generated using $J_{\text{GMO}} = -1.05$ mb and $a_{\pi^-p} = 0.085 \mu^{-1}$. It is important to stress that any reasonable set [32] could be used and that the minimum value for $g^2/4\pi$ depends only weakly upon the chosen values. Moreover, these choices have a negligible effect on our results for the resonance spectrum.

Given the above choices of J_{GMO} and a_{π^-p} , Table III shows the sensitivity of our fits to the value of $g^2/4\pi$. The most important difference between this mapping and our previous result [2] is the consistency of the optimal value of $\pi N N$ coupling found from the constraints and all charge channels. A problem once evident in Ref. [2], in the charge-exchange channel, has now disappeared.

C. Lesser structure

There has been some criticism [3] of our method of analysis, based upon the absence of some lesser (less than 4-star) structures in the Virginia Polytechnic Institute (VPI) solutions. It has been argued that this is the result of inflexibility in the energy-dependent forms which we use. We have previously searched for missing structure by iterating between single-energy and global fits, examining each iteration for evidence of systematic deviations between the resultant partial waves.

In order to explore this question more carefully, we have performed an additional search for (localized) missing structures, implementing the following strategy. We have assumed a product S matrix of the form

$$S = S_{\text{FA93}} S_P, \quad (5)$$

where S_{FA93} is the solution [2] used in our recent determinations of $g^2/4\pi$, and S_P was taken to have the form:

$$S_P = (1 + 2iT_R) \begin{pmatrix} 1 + iK_B \\ 1 - iK_B \end{pmatrix} \quad (6)$$

with

TABLE III. Table of χ^2 values for different choices of the pion-nucleon coupling used in the analysis of $\pi^\pm p$ elastic scattering and charge-exchange (CXS) data. The number of data (or constraints) is given in brackets.

Solution	$g^2/4\pi$	Data (21220)	Constraints (496)	π^+ (10190)	π^- (9350)	CXS (1680)
E337	13.37	47 921	709	23 269	19 935	4717
E350	13.50	46 776	527	22 759	19 466	4551
E363	13.63	46 127	410	22 557	19 108	4462
E375	13.75	45 919	352	22 599	18 877	4443
E387	13.87	46 030	367	22 799	18 775	4456
E400	14.00	46 483	452	23 176	18 789	4518
χ_{\min}^2		45 918	355	22 552	18 766	4435
$g^2/4\pi_{\min}$		13.77	13.79	13.69	13.93	13.77
$\Delta(g^2/4\pi_{\min})$		0.01	0.03	0.02	0.02	0.03

TABLE IV. Single-energy (binned) fits of combined $\pi^\pm p$ elastic scattering and charge-exchange data, and χ^2 values. N_{prm} is the number parameters varied in the single-energy fits, and χ_E^2 is given by the energy-dependent fit, SM95, over the same energy interval.

T_{lab} (MeV)	Range (MeV)	N_{prm}	$\chi^2/\pi N$ data	χ_E^2	T_{lab} (MeV)	Range (MeV)	N_{prm}	$\chi^2/\pi N$ data	χ_E^2
30	26–33	4	242/136	290	820	813–827	26	398/304	482
47	45–49	4	72/81	108	868	864–870	32	277/195	407
66	61–69	4	189/122	245	888	886–890	33	173/144	309
91	89–92	4	79/73	98	902	899–905	34	550/416	852
124	121–126	6	74/61	88	927	923–930	36	240/200	373
145	141–147	6	36/42	50	962	953–971	36	384/299	557
170	165–174	6	87/67	95	1000	989–1015	38	689/423	865
193	191–194	6	45/54	52	1030	1022–1039	39	284/272	400
217	214–220	6	69/59	152	1044	1039–1049	40	357/243	538
238	235–240	6	79/72	95	1076	1074–1078	43	221/218	427
266	262–270	7	117/88	163	1102	1099–1103	44	226/173	335
292	291–293	8	148/129	222	1149	1147–1150	44	325/210	459
309	306–310	8	169/140	227	1178	1165–1192	44	763/394	985
334	332–335	9	96/58	133	1210	1203–1216	44	286/233	372
352	351–352	9	79/110	148	1243	1237–1248	44	452/283	641
389	387–390	9	30/28	101	1321	1304–1337	44	728/401	950
425	424–425	10	146/139	206	1373	1371–1375	44	308/166	581
465	462–467	15	355/120	466	1403	1389–1417	44	547/408	783
500	499–501	15	159/136	185	1458	1455–1460	44	280/258	448
518	515–520	16	101/79	149	1476	1466–1486	44	486/323	648
534	531–535	19	134/128	203	1570	1554–1586	46	831/546	1125
560	557–561	19	331/151	570	1591	1575–1606	46	425/336	647
580	572–590	19	369/286	460	1660	1645–1674	46	553/391	821
599	597–600	22	250/151	502	1720	1705–1734	46	398/279	528
625	622–628	23	126/95	199	1753	1739–1766	46	660/439	863
662	648–675	23	584/352	750	1838	1829–1845	46	461/290	709
721	717–725	25	203/169	300	1875	1852–1897	46	989/682	1358
745	743–746	25	164/100	293	1929	1914–1942	46	840/501	1297
765	762–767	26	190/169	330	1970	1962–1978	46	477/271	688
776	774–778	26	226/155	318	2026	2014–2037	46	414/320	794
795	793–796	26	206/165	319					

$$T_R = \frac{\Gamma_{\pi N}/2}{W_R - W - i\Gamma/2}, \quad (7)$$

where $\Gamma_{\pi N} = \rho_e \gamma_e$ and $\Gamma_i = \rho_i \gamma_i$. The total width Γ is given by the sum of elastic ($\Gamma_{\pi N}$) and inelastic (Γ_i) widths with phase-space factors, $\rho_{e,i}$, normalized to unity at $W = W_R$. In the above, K_B is expressed as $\gamma_B |T_R|^2$ (in order to keep the effect localized).

We mapped $\chi^2(W_R, \gamma_B)$ for various combinations of the constants γ_e and γ_i . W_R was varied from 1.4 to 2.3 GeV, in increments of 25 MeV, and γ_B was varied from -10 to 10 in increments of 5. This was done for each partial wave. A few candidates for extra structure were found in this way. Once identified, these added structures were included in a fit constrained by dispersion relations.

D. Resonance parameter extraction

The resonance spectrum for our fit was extracted in the customary fashion. A Breit-Wigner form plus background was used to fit partial waves containing structure over a selected range of energies. The precise form is given by

$$S = 1 + 2iT = (1 + 2iT_R) \eta_B e^{2i\delta_B} \quad (8)$$

with T_R defined as above. The main requirement on the phase-space factors is that ρ_e should be proportional to $(W - M - \mu)^{l+1/2}$ at threshold, which allows for many possible choices. For the background we used

$$\delta_B = \delta_B^r + \alpha(W_R - W) \quad (9)$$

with $\eta_B = \cos(\rho_B)$. To get initial values for the resonance fitting, we implemented the speed plot (speed = $|dT/dW|$) advocated by Höhler [6,7]. All 4-star resonances show clear “speed bumps” allowing the extraction of initial parameters.

The values for extracted resonance parameters ($W_R, \Gamma_{\pi N}, \Gamma$) were quite sensitive to the choice of phase-space factors, especially for those resonances near threshold. For the P_{33} in particular, it was possible to obtain reasonable fits for a variety of assumed factors. We ultimately adopted the form

$$\rho_e = \left(\frac{q}{q_R}\right)^{2l+1} \left(\frac{q_R^2 + X^2}{q^2 + X^2}\right)^l, \quad (10)$$

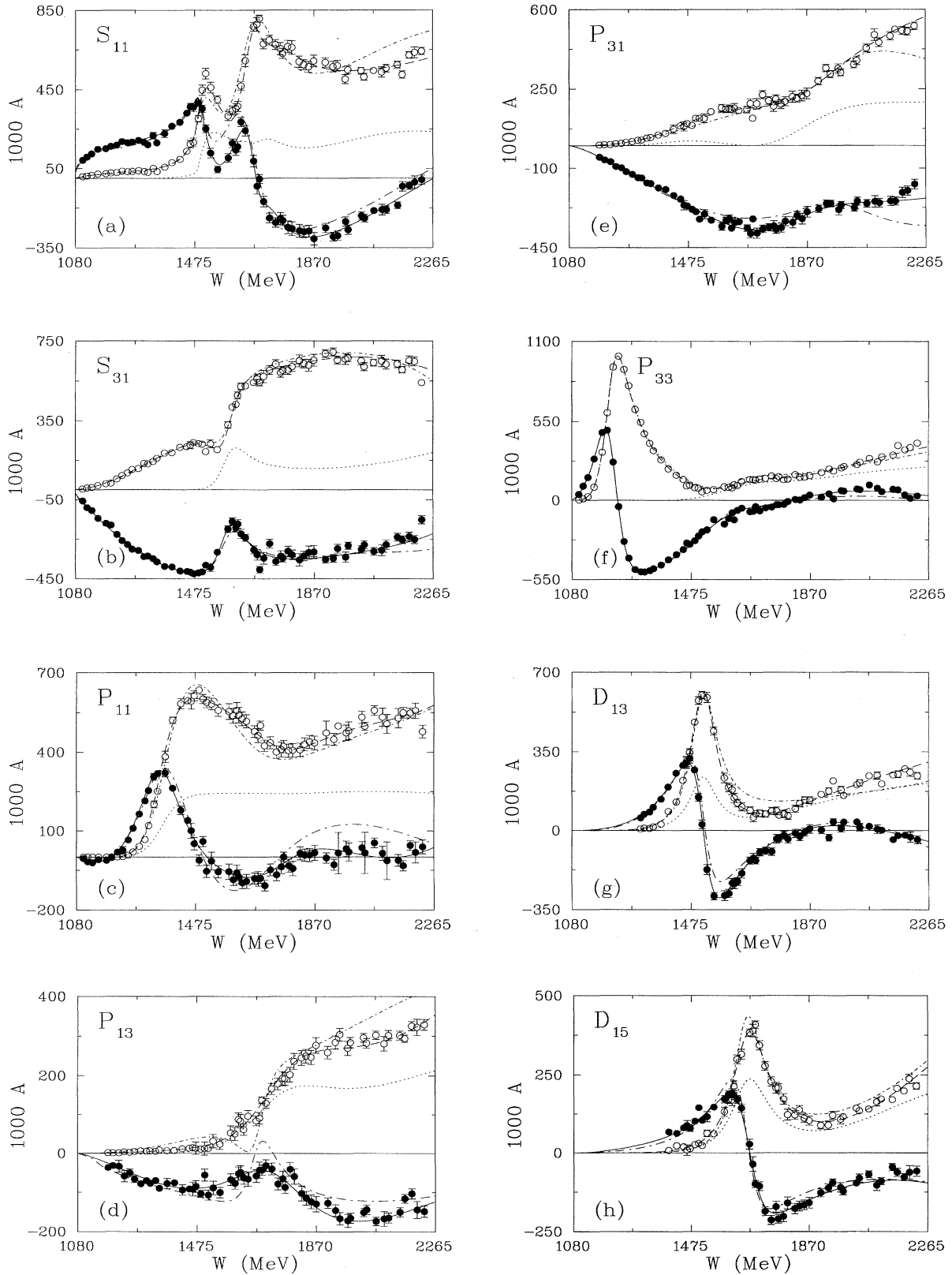


FIG. 2. Partial-wave amplitudes ($L_{2l,2l}$) from 0 to 2.1 GeV. Solid (dashed) curves give the real (imaginary) parts of amplitudes corresponding to the SM95 solution. The real (imaginary) parts of single-energy solutions are plotted as filled (open) circles. The previous SM90 solution [1] is plotted with long dash-dotted (real part) and short dash-dotted (imaginary part) lines. The dotted curve gives the value of $\text{Im}T - T^*T$. All amplitudes have been multiplied by a factor of 10^3 and are dimensionless.

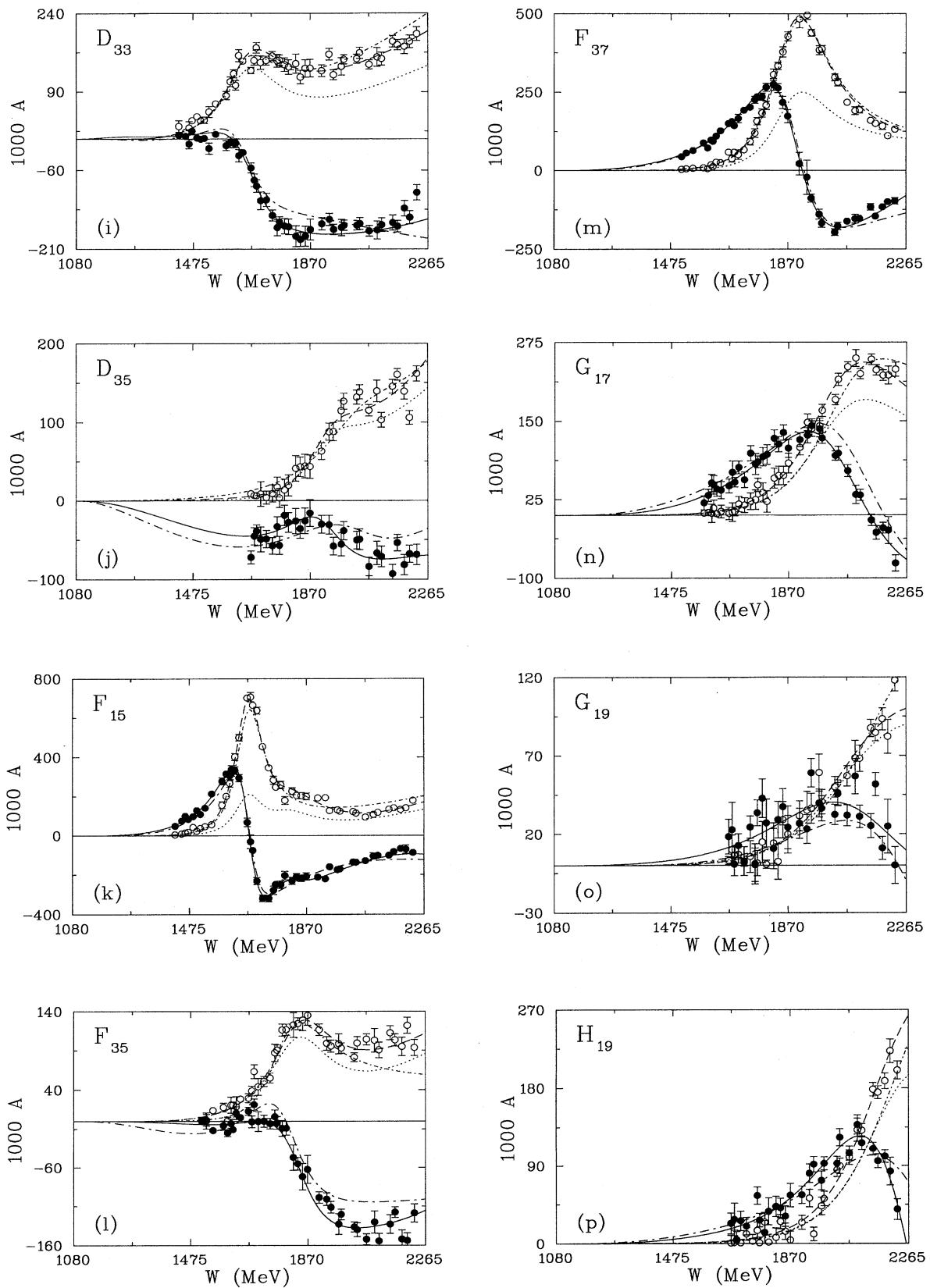


FIG. 2. (Continued.)

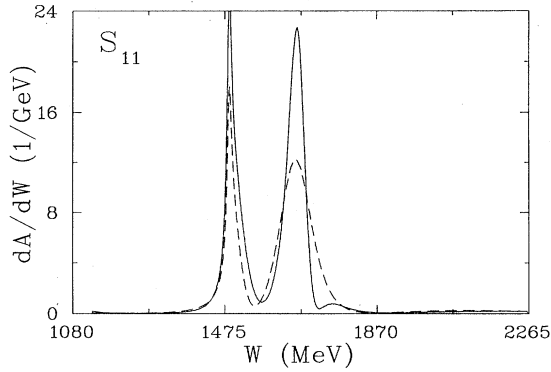


FIG. 3. Speed plot of the S_{11} amplitude. The solid (dashed) line gives the result for solution SM95 (SM90) [1].

where q and q_R are the center-of-mass and resonance momenta. This introduces a cutoff parameter, X , but seems to yield, for most 4-star resonances, values consistent with previous Particle Data Group (PDG) [33] determinations. We plan a more refined analysis of the $P_{33}(1232)$ resonance region once we receive the data of Refs. [26–29]. It is hoped that these new measurements will help to resolve discrepancies existing in the current database for this energy region.

E. Complex plane mapping: poles and zeros

Since the form used in our energy-dependent fits can be analytically continued to complex energies, it is straightforward to locate the complex energy positions for the poles and zeros which influence the on-shell behavior of the amplitudes. We generate complex-plane contour plots of $\ln(|T|^2)$ and pick a starting energy near the pole/zero. We then use a Newton-Raphson algorithm to “home in” on the structure. Results for the pole positions (and residues) are given in the next section.

IV. RESULTS OF THE PARTIAL-WAVE ANALYSIS

The overall quality of our solution (SM95) is displayed in Table I, along with a number of our previous results. Single-energy solutions were produced up to 2026 MeV. For these single-energy solutions, starting values for the partial-wave amplitudes and their (fixed) energy derivatives were obtained from the energy-dependent fit. The scattering database was supplemented with a constraint on each varied amplitude. Constraint errors were taken to be 0.02 added in quadrature to 5% of the amplitude. Such constraints are essential to prevent the solutions from “running away” when a bin is sparsely populated with scattering data, but have little effect when sufficient data exists. In Table IV we compare the energy-dependent and single-energy fits to the data. These solutions are displayed graphically in Fig. 2. Here we also compare with the previous solution SM90. Some of the largest changes are seen in S_{11} (near the η cusp), in P_{13} (at intermediate energies), and in P_{11} (at higher energies).

Our search for lesser structures, as described in Sec. III C, revealed only three possibilities for obtaining a significantly improved fit. After inclusion into the main analysis, we determined that only two of these lesser structures, in the S_{11} and F_{15} partial waves, remained significant enough to keep

in our final fit. These can be seen as small “bumps” on the high-energy shoulders of the $S_{11}(1650)$ and $F_{15}(1680)$ resonances. The S_{11} structure is also evident in the speed plot of Fig. 3.

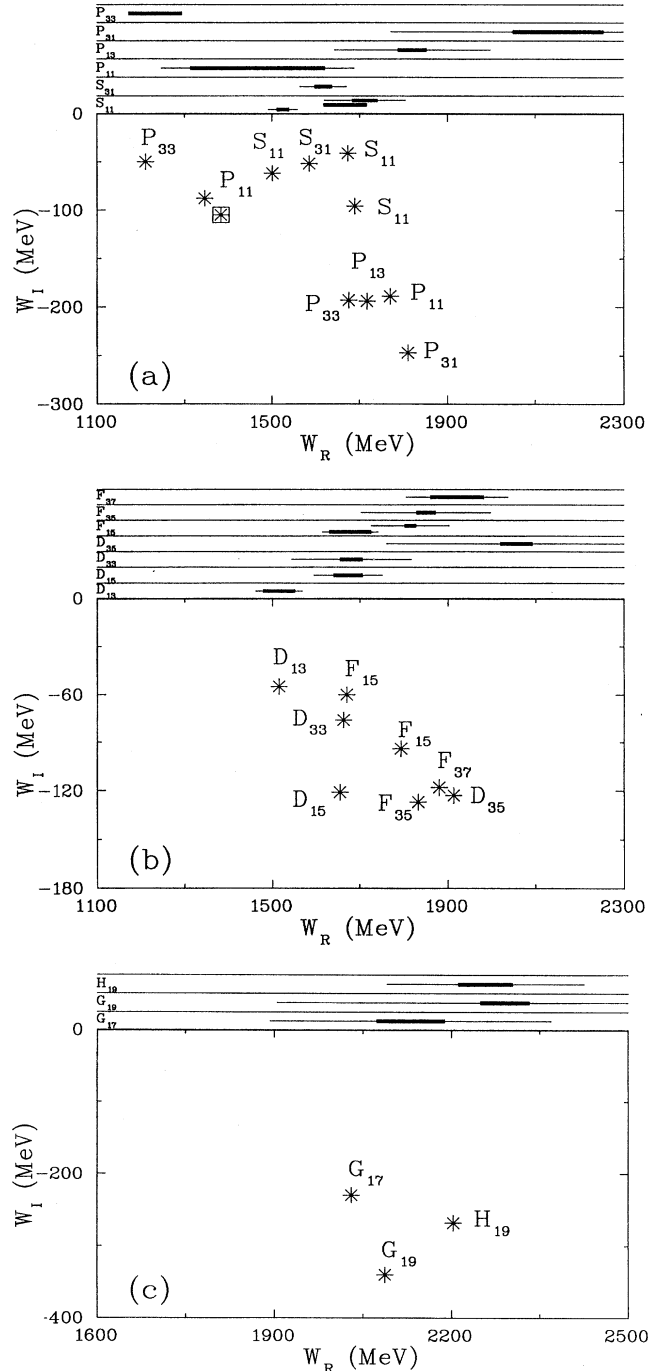


FIG. 4. Comparison of complex plane and Breit-Wigner fits for resonances found in solution SM95. Complex plane poles are plotted as stars (the boxed star denotes a second-sheet pole). W_R and W_I give real and imaginary parts of the center-of-mass energy. The total (elastic) widths are denoted by narrow (wide) bars for each resonance. (a) S - and P -wave resonances; (b) D - and F -wave resonances; (c) G - and H -wave resonances.

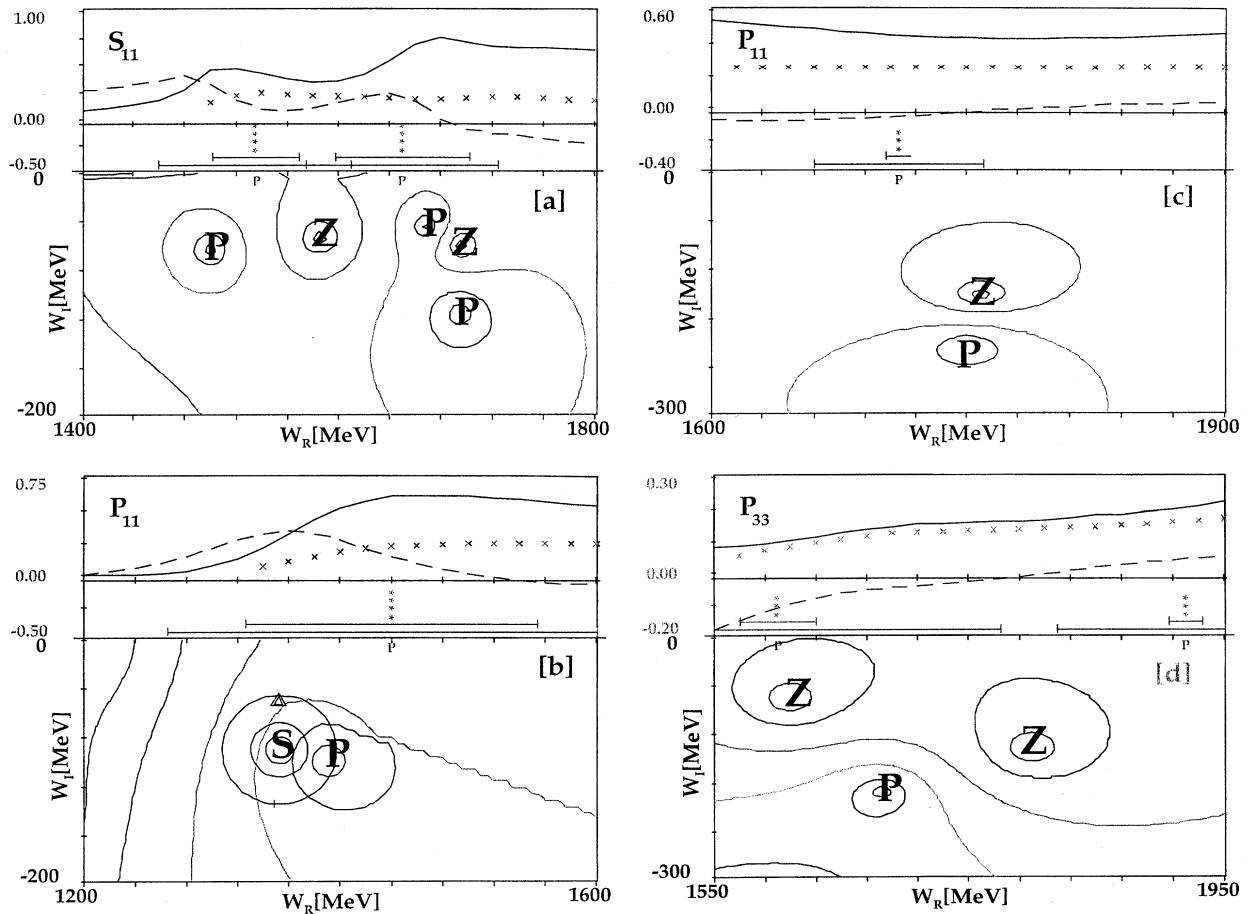


FIG. 5. Complex plane pole/zero plot for the (a) S_{11} , (b) low-energy P_{11} , (c) high-energy P_{11} , and (d) P_{33} partial-wave amplitudes. P and Z denote the pole and zero positions. S indicates a second-sheet pole. Stars locate nearby PDG resonance positions and the underlying bars give the PDG values for the elastic and full widths.

Pole positions and the associated Breit-Wigner parameters are presented graphically in Fig. 4, and are listed in Tables V and VI. PDG values are also given for comparison. We have not attempted to associate the added structures in S_{11} and F_{15} with any specific PDG designation. A structure found in P_{13} was likewise left “unnamed.”

We are able to resolve all 4-star structures listed by the PDG within our energy range. We also determined structure in the speed plots for P_{33} around 1800 MeV, and for P_{31} near 1400 MeV. Neither of these were resolvable via a Breit-Wigner fit. The difficulty with these unresolved structures can be seen in Fig. 5, which reveals a rather complicated interference between nearby zeros and poles. Many of the weaker structures appear as pole-zero combinations, with a zero lying between the pole and the physical axis.

V. COMPARISONS AND DISCUSSION

As we find structures associated with all 4-star resonances in our energy range, we can claim qualitative agreement with the Karlsruhe, CMB, and Kent State analyses. The P_{13} result is difficult to interpret. We find a pole position close to the CMB value but the Breit-Wigner fit results in a resonance energy between the 4-star $P_{13}(1720)$ and 1-star $P_{13}(1910)$.

Our two additional resonances, found in sweeping a Breit-Wigner form through the partial-wave amplitudes, could possibly be related to PDG 1- and 2-star resonances found previously in the S_{11} and F_{15} amplitudes. The Karlsruhe group reported a structure [denoted as the $F_{15}(2000)$ 2-star resonance] at 1882 MeV, not far from our value. The elasticity we found is also similar to that found by the Karlsruhe and Kent State groups. The next S_{11} resonance reported above the $S_{11}(1650)$ is the 1-star $S_{11}(2090)$. Our structure appears about 150 MeV below this. It is interesting to note that Höhler [7] found a similar structure in his speed plot of the KA84 solution.

The PDG 3-star $D_{13}(1700)$ resonance is not evident in the present analysis. The Kent State group found an elasticity consistent with zero for this resonance. The photocouplings to the $D_{13}(1700)$ are also consistent with zero in the most recent PDG estimates. If this resonance exists, it remains very difficult to detect. We do see the 3-star $P_{33}(1600)$, though our pole position is quite different from the Karlsruhe and CMB values. The resonance energy estimates, from the Karlsruhe, CMB, and Kent State groups, also span a wide range.

In summary, we have found that our present analysis

TABLE V. Masses, half-widths ($\Gamma/2$), and values for ($\Gamma_{\pi N}/\Gamma$) are listed for isospin-1/2 baryon resonances, along with associated pole positions from our solution SM95 (second sheet poles are denoted by a †). Corresponding residues are given as a modulus and phase (in degrees). Average values from the Review of Particle Properties [33] are given in square brackets.

Resonance (* rating)	W_R (MeV)	$\Gamma/2$ (MeV)	$\Gamma_{\pi N}/\Gamma$	Pole (MeV)	Residue (MeV, °)
$P_{11}(1440)$	1467	220	0.68	1346 - i 88 (1383 - i 105)†	(42, -101) (92, -54)†
****	[1440]	[175]	[0.65]		
$D_{13}(1520)$	1515	53	0.61	1515 - i 55	(34, 7)
****	[1520]	[60]	[0.55]		
$S_{11}(1535)$	1535	33	0.31	1501 - i 62	(31, -12)
****	[1535]	[75]	[0.45]		
$S_{11}(1650)$	1667	45	\approx 1.0	1673 - i 41	(22, 29)
****	[1650]	[75]	[0.70]		
S_{11}	1712	92	0.27	1689 - i 96	(72, -85)
$D_{15}(1675)$	1673	77	0.38	1663 - i 76	(29, -6)
****	[1675]	[75]	[0.45]		
$F_{15}(1680)$	1678	63	0.68	1670 - i 60	(40, 1)
****	[1680]	[65]	[0.65]		
$P_{11}(1710)$	—	—	—	1770 - i 189	(37, -167)
****	[1710]	[50]	[0.15]		
P_{13}	1820	177	0.16	1717 - i 194	(39, -70)
F_{15}	1814	88	0.10	1793 - i 94	(27, -56)
$G_{17}(2190)$	2131	238	0.23	2030 - i 230	(46, -23)
****	[2190]	[225]	[0.15]		
$H_{19}(2220)$	2258	167	0.26	2203 - i 268	(68, -43)
****	[2220]	[200]	[0.15]		
$G_{19}(2250)$	2291	386	0.10	2087 - i 340	(24, -44)
**	[2250]	[200]	[0.10]		

TABLE VI. Parameters for isospin-3/2 baryon resonances. Notation as in Table V.

Resonance (* rating)	W_R (MeV)	$\Gamma/2$ (MeV)	$\Gamma_{\pi N}/\Gamma$	Pole (MeV)	Residue (MeV, °)
$P_{33}(1232)$	1233	57	\approx 1.0	1211 - i 50	(38, -22)
****	[1232]	[60]	[0.994]		
$P_{33}(1600)$	—	—	—	1675 - i 193	(52, 14)
***	[1600]	[175]	[0.17]		
$S_{31}(1620)$	1617	54	0.29	1585 - i 52	(14, -121)
****	[1620]	[75]	[0.25]		
$D_{33}(1700)$	1680	136	0.16	1655 - i 121	(16, -12)
****	[1700]	[150]	[0.15]		
$F_{35}(1905)$	1850	147	0.12	1832 - i 127	(12, -4)
****	[1905]	[175]	[0.10]		
$P_{31}(1910)$	2152	380	0.26	1810 - i 247	(53, -176)
****	[1910]	[125]	[0.22]		
$D_{35}(1930)$	2056	295	0.11	1913 - i 123	(8, -47)
***	[1930]	[175]	[0.15]		
$F_{37}(1950)$	1921	116	0.49	1880 - i 118	(54, -17)
****	[1950]	[150]	[0.38]		

gives all the dominant structures found in earlier works, along with a couple of new ones which may be related to previous 1- or 2-star states. We also found the value of $g^2/4\pi$ to be more consistently determined by individual charge channels and the constraints than was the case in our first set [2] of χ^2 maps. These amplitudes will be used as input for our upcoming analysis of pion photoproduction data. Results for the new S_{11} and F_{15} resonances will be especially interesting, as these states presently have no assigned photocoupling estimates in the Review of Particle Properties.

This reaction is incorporated into the SAID program [34], which is maintained at Virginia Tech.

ACKNOWLEDGMENTS

The authors express their gratitude to I. G. Alekseev, A. Badertscher, B. Bassalleck, J. T. Brack, D. V. Bugg, J.-P. Egger, E. Friedman, G. Jones, V. V. Kulikov, I. V. Lopatin, C. A. Meyer, R. Minehart, B. M. K. Nefkens, D. Počanić, R. A. Ristinen, M. Sadler, M. Sevier, G. R. Smith, and J. Stasko for providing experimental data prior to publication or clarification of information already published. We also acknowledge useful communications with G. Höhler. I.S. acknowledges the hospitality extended by the Physics Department of Virginia Tech. This work was supported in part by the U.S. Department of Energy Grant No. DE-FG05-88ER40454 and a NATO Collaborative Research Grant No. 921155U.

-
- [1] R. A. Arndt, L. Zhujun, L. D. Roper, R. L. Workman, and J. M. Ford, *Phys. Rev. D* **43**, 2131 (1991).
- [2] R. A. Arndt, R. L. Workman, and M. M. Pavan, *Phys. Rev. C* **49**, 2729 (1994).
- [3] G. Höhler (private communication).
- [4] R. A. Arndt, J. M. Ford, and L. D. Roper, *Phys. Rev. D* **32**, 1085 (1985).
- [5] G. Höhler, in *Pion-Nucleon Scattering*, edited by H. Schopper, Landolt-Börnstein, Vol. **I/9b2** (Springer-Verlag, Berlin, 1983).
- [6] G. Höhler and A. Schulte, Report No. TTP 92-27, Karlsruhe, 1992.
- [7] G. Höhler, in Proceedings of the 5th Meson-Nucleon Symposium, Boulder, Colorado, 1993, edited by B. M. K. Nefkens and M. Clajus [*πN Newslett.* **9**, 1 (1993)].
- [8] R. L. Kelly and R. E. Cutkosky, *Phys. Rev. D* **20**, 2782 (1979); R. E. Cutkosky, R. E. Hendrick, J. W. Alcock, Y. A. Chao, R. G. Lipes, J. A. Sandusky, and R. L. Kelly, *ibid.* **20**, 2804 (1979); R. E. Cutkosky, C. P. Forsyth, R. E. Hendrick, and R. L. Kelly, *ibid.* **20**, 2839 (1979); R. E. Cutkosky, C. P. Forsyth, J. B. Babcock, R. L. Kelly, and R. E. Hendrick, in *Proceedings of 4th International Conference on Baryon Resonances*, Toronto, Canada, 1980, edited by N. Isgur (World Scientific, Singapore, 1981), p. 19.
- [9] D. M. Manley and E. M. Saleski, *Phys. Rev. D* **45**, 4002 (1992).
- [10] The 1-, 2-, and 3-star rating of data is described in Ref. [1]. Of the data rated in 1987, only 2- and 3-star data are included in analyses. Unrated data are included unless they have been “flagged” for deletion from analyses. It should be noted that these flagged data have been retained in our database.
- [11] B. M. Abramov, S. A. Bulychev, I. A. Dukhovskoi, V. V. Kishkurno, Y. S. Krestnikov, A. B. Krutenkova, V. V. Kulikov, M. A. Matsyuk, P. A. Murat, S. V. Proshin, I. A. Radkevich, N. G. Tkatch, E. N. Turdakina, and V. S. Fedorets, *Yad. Fiz.* **54**, 550 (1991) [*Phys. At. Nucl. (former Sov. J. Nucl. Phys.)* **54**, 332 (1991)].
- [12] I. G. Alekseev, P. E. Budkovsky, V. P. Kanavets, L. I. Koroleva, I. I. Levintov, V. I. Martynov, B. V. Morozov, V. M. Nesterov, V. V. Platonov, V. V. Ryltsov, V. A. Sakharov, D. N. Svirida, A. V. Soskov, A. D. Sulimov, and V. V. Sumachev, *Nucl. Phys.* **B348**, 257 (1991).
- [13] A. Bosshard, A. Amsler, M. Döbeli, M. Doser, M. Schaad, J. Riedlberger, P. Truöl, J. A. Bistirlich, K. M. Crow, S. Ljungfelt, C. A. Meyer, B. van den Brandt, J. A. Konter, S. Mango, D. Renker, J. F. Loude, J. P. Perroud, R. P. Haddock, and D. I. Sober, *Phys. Rev. D* **44**, 1962 (1991).
- [14] J. T. Brack, P.-A. Amaudruz, D. F. Ottewell, G. R. Smith, M. Kermani, M. Pavan, D. Vetterli, R. A. Ristinen, S. Höibråten, M. D. Kohler, J. J. Kraushaar, B. J. Kriss, J. Jaki, M. Metzler, and E. F. Gibson, *Phys. Rev. C* **51**, 929 (1995).
- [15] E. Friedman, A. Goldring, G. J. Wagner, A. Altman, R. R. Johnson, O. Meirav, M. Hanna, and B. K. Jennings, *Phys. Lett. B* **254**, 40 (1991).
- [16] E. Friedman, M. Paul, M. Schechter, A. Altman, B. K. Jennings, G. J. Wagner, N. Fazel, R. R. Johnson, N. Suen, and Z. Fraenkel, *Phys. Lett. B* **302**, 18 (1993); E. Friedman (private communication).
- [17] M. Sadler (private communication).
- [18] C. Joram, M. Metzler, J. Jaki, W. Kluge, H. Matthäy, R. Wieser, B. M. Barnett, R. Bilger, H. Clement, K. Föhl, K. Heitlinger, S. Krell, and G. J. Wagner, *Phys. Rev. C* **51**, 2159 (1995).
- [19] I. V. Lopatin, V. V. Abaev, N. A. Bazhanov, V. S. Bekrenev, Yu. A. Beloglazov, E. A. Filimonov, A. I. Kovalyov, N. G. Kozlenko, S. P. Kruglov, A. A. Kulbardis, L. V. Lapochkina, V. V. Polyakov, V. A. Shchedrov, A. V. Shvedchikov, V. V. Sumachev, I. I. Tkach, and V. Yu. Trautman, *Nucl. Phys.* **A567**, 882 (1994).
- [20] C. Joram, M. Metzler, J. Jaki, W. Kluge, H. Matthäy, R. Wieser, B. M. Barnett, H. Clement, S. Krell, and G. J. Wagner, *Phys. Rev. C* **51**, 2144 (1995).
- [21] D. Počanić (private communication); R. Minehart (private communication).
- [22] J. Stasko, Ph.D. thesis, University of New Mexico, 1993; B. Bassalleck (private communication).
- [23] I. Supek, D. B. Barlow, W. J. Briscoe, J. F. Davis, G. J. Kim, D. W. Lane, A. Mokhtari, B. M. K. Nefkens, C. Pillai, M. E. Sadler, C. J. Seftor, M. F. Taragin, and J. A. Wightman, *Phys. Rev. D* **47**, 1762 (1993).
- [24] V. V. Sumachev, V. V. Abaev, N. A. Bazhanov, V. S. Bekrenev, Yu. A. Beloglazov, A. I. Kovalev, N. G. Kozlenko, A. A. Kulbardis, I. V. Lopatin, V. Yu. Trautman, E. A. Filimonov, V. A. Shchedrov, I. G. Alekseev, B. M. Bobchenko, P. E. Budkovsky, V. V. Zhurkin, V. P. Kanavets, L. I. Koroleva, V. I. Martynov, B. V. Morozov, V. M. Nesterov, V. V. Platonov, V. V. Ryltsov,

- V. A. Sakharov, D. N. Svirida, and A. D. Sulimov, submitted to *Yad. Fiz.* [*Phys. At. Nucl.* (former *Sov. J. Nucl. Phys.*)]; SPNPI Report-1992, St. Petersburg, 1994; I. G. Alekseev (private communication).
- [25] R. Wieser (private communications).
- [26] M. M. Pavan, Ph.D. thesis, University of British Columbia, 1995.
- [27] B. J. Kriss, R. A. Ristinen, S. Høibråten, M. Holcomb, M. D. Kohler, J. J. Kraushaar, S. P. Parry, A. Saunders, W. R. Smythe, C. L. Morris, M. Rawool-Sullivan, R. M. Whitton, J. T. Brack, E. F. Gibson, and J. L. Langenbrunner, in *Proceedings of the 5th Meson-Nucleon Symposium*, Boulder, Colorado, 1993, edited by B. M. K. Nefkens and M. Clajus [*πN Newslett.* **8**, 17 (1993)].
- [28] G. R. Smith *et al.*, TRIUMF Experiment 560, “Low energy πp analyzing powers with CHAOS,” TRIUMF Annual Report, Scientific Activities, 1993 and 1994; G. R. Smith (private communication).
- [29] J. R. Comfort *et al.*, LAMPF Experiment 1178, “Polarization asymmetry measurements for $\pi^- p \rightarrow \pi^0 n$ between 45 and 265 MeV”; J. R. Comfort (private communication).
- [30] B. Tromborg, S. Waldenstrom, and I. Overbo, *Phys. Rev. D* **15**, 725 (1977); *Helv. Phys. Acta.* **51**, 584 (1978).
- [31] R. Koch, *Nucl. Phys.* **A448**, 707 (1986).
- [32] Preliminary results from a pionic atom experiment suggest a value of $(0.0873 \pm 0.0007) \mu^{-1}$ for $(2a_1 + a_3)/3$ and $(-0.096 \pm 0.008) \mu^{-1}$ for $(a_1 - a_3)/3$, J.-P. Egger (private communication).
- [33] L. Montanet, R. M. Barnett, D. E. Groom, T. G. Trippe, C. G. Wohl, H. Murayama, J. Stone, J. J. Hernandez, F. C. Porter, R. J. Morrison, A. Manohar, M. Anduilar-Benitez, C. Caso, R. L. Crawford, M. Roos, N. A. Törnqvist, K. G. Hayes, G. Höhler, S. Kawabata, D. M. Manley, K. Olive, R. E. Shrock, S. Eidelman, R. H. Schindler, A. Gurtu, K. Hikasa, G. Conforto, R. L. Workman, and C. Grab, *Phys. Rev. D* **50**, 1173 (1994).
- [34] Those with access to TELNET can run the SAID program with a link to VTINTE.PHYS.VT.EDU (128.173.176.61). The login (password) is PHYSICS (QUANTUM). The user may view the current database and compare our solutions to those of other groups. A WWW server is also available (<http://clsaid.phys.vt.edu>).